Title	Single Crystalline, Non-stoichiometric Cocrystals of Hydrogen-Bonded Organic Frameworks
Author(s)	Hashimoto, Taito; Oketani, Ryusei; Nobuoka, Masaki et al.
Citation	Angewandte Chemie - International Edition. 2023, 62(1), p. e202215836
Version Type	AM
URL	https://hdl.handle.net/11094/92730
rights	© 2022 Wiley-VCH GmbH. & Co. KGaA.
Note	

Single Crystalline, Non-stoichiometric Cocrystals of Hydrogen-Bonded Organic Frameworks

Taito Hashimoto,[a] Ryusei Oketani,[a] Masaki Nobuoka,[b] Shu Seki,[b] Ichiro Hisaki*[a]

[a] T. Hashimoto, Dr. R. Oketani, Prof. Dr. I. Hisaki
Division of Chemistry, Graduate School of Engineering Science
Osaka University
1-3 Machikaneyama, Toyonaka, Osaka 560-8531, Japan.
E-mail: i.hisaki.es@osaka-u.ac.jp (I.H.)
[b] M. Nobuoka, Prof. Dr. S. Seki
Department of Molecular Engineering, Graduate School of Engineering
Kyoto University
Nishikyo-ku, Kyoto, 615-8510, Japan.

Supporting information for this article is given via a link at the end of the document.

Abstract: Porous frameworks composed of non-stoichiometrically mixed multicomponent molecules attract much attention from a functional viewpoint. however, their designed preparation and precise structural characterization remain challenging. Herein, we demonstrate that cocrystallization of tetrakis(4-carboxyphenyl)hexahydropyrene and pyrene derivatives (**CP-Hp** and **CP-Py**, respectively) yields non-stoichiometric mixed frameworks through networking *via* hydrogen bonding. The composition ratio of **CP-Hp** and **CP-Py** in the framework was determined by single crystalline X-ray crystallographic analysis, indicating that the mixed frameworks were formed over a wide range of composition ratios. Furthermore, microscopic Raman spectroscopy on the single crystal indicates that the components are not uniformly distributed such as ideal solid solution, but are done gradationally or inhomogeneously.

Non-stoichiometrically mixed multicomponent cocrystals have been a topic of interest to materials scientists because their functionalities can be fine-tuned and/or conflated by changing the components and their ratio and because, in some cases, a totally new functionality can be created.[1-3] Thus far, numerous multicomponent organic crystals have been obtained on the basis of supramolecular approaches using non-covalent interactions such as charge transfer (CT) interactions,[4] hydrogen bonds,[5-7] and halogen bonds,[8] as well as dative bonds[9] and dynamic covalent bonds.[10] Such crystals have been used in luminescent materials,[11] selective absorbents,[9] and pharmaceutical products.[12]

In this study, we became interested in porous crystalline framework materials composed of non-stoichiometric multiple components. In a pioneering work, Yaghi and coworkers prepared multicomponent metal–organic frameworks (MOFs) with various terephthalates and demonstrated that the multicomponent MOFs exhibit selective uptake of CO_2 over CO, which were not achieved by pristine MOF-5.[9] Unlike MOFs, porous molecular crystals formed through hydrogen bonds (known as hydrogen-bonded organic frameworks, HOFs)[13-18] are difficult to construct from a non-stoichiometric mixture of component molecules, although stoichiometric multicomponent HOFs were prepared.[19-24]

In general, HOFs are obtained by simple recrystallization as single crystals with a suitable size and quality for single-crystal X-ray diffraction analysis. The recrystallization process, however, excludes minor component molecules from the crystalline system even if their molecular sizes and shapes match with each other. Thus far, a handful of non-stoichiometric multicomponent HOFs have been constructed.[4,25] However, a precise crystallographic analysis could not be conducted except for powder X-ray diffraction of bulk precipitates. Constructing well-defined non-stoichiometric cocrystalline frameworks with the desired composition ratio remains challenging.

Herein, we demonstrate, for the first time, the construction and precise crystallographic characterization of non-stoichiometric cocrystalline HOFs. The frameworks are composed of tetrakis(4-carboxyphenyl)hexahydropyrene and pyrene derivatives (**CP-Hp** and **CP-Py**, respectively) with various composition ratios (Figure 1). Although their pristine compounds gave no cocrystals, we found that the derivatives possessing four carboxyphenyl groups successfully form mixed frameworks through H-bonding of the peripheral carboxy groups.[26-28] The composition ratio in the crystals shows a good correlation with that in the initial solution used for recrystallization. Moreover, microscopic Raman spectroscopic analysis of single crystals revealed that both the **CP-Hp** and **CP-Py** components are incorporated into the single crystal, and are not distributed uniformly but instead gradationally and/or inhomogeneously. This is the first example to reveal distribution of the nonstoichiometric components in single crystals of HOFs.

CP-Hp and **CP-Py**, [29] synthesized according to Scheme S1, were recrystallized independently to give single component HOFs **CP-Hp-1** and **CP-Py-1**, respectively (Figure 2a,b).[30] In both structures, the carboxy groups of the molecules form a self-complementary dimer through H-bonds with an O···O distance of 2.61–2.63 Å for **CP-Hp-1** and 2.62–2.63 Å for **CP-Py-1** to give ***sql***-topological two-dimensional (2D) layered motifs with a rhombic void. In the void, molecules of *o*DCB are accommodated with a host/guest ratio of 1:4 (Figure 2d). The 2D

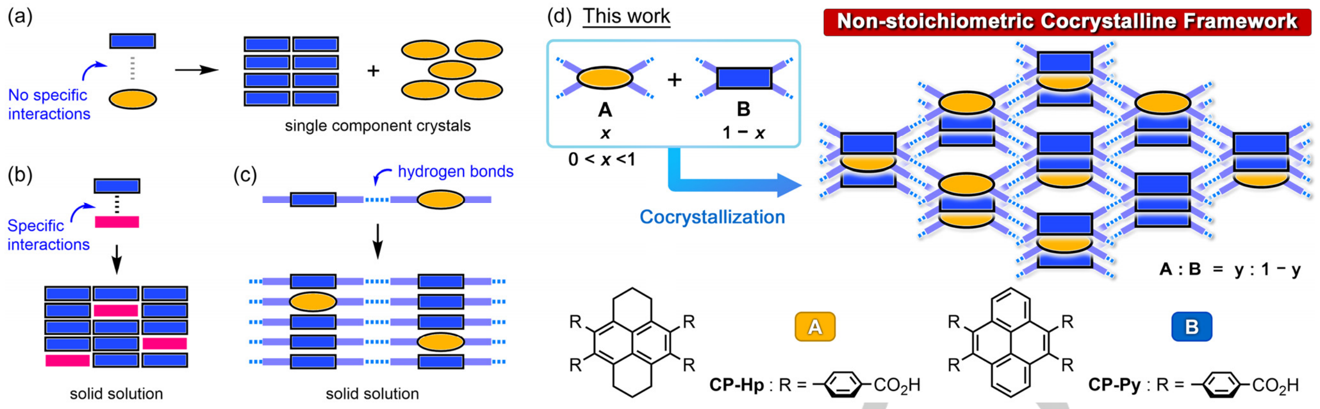

Figure 1. Concept of non-stoichiometric cocrystalline frameworks. (a) Spontaneous resolution for component molecules A and B without specific interactions. (b) Solid-solution formation through strong interaction between pristine molecules. (c) Solid-solution formation through hydrogen bonds between modules. (d) Construction of a 2D networked hydrogen-bonded solid-solution framework using hexahydropyrene and pyrene derivatives **CP-Hp** and **CP-Py**, respectively.

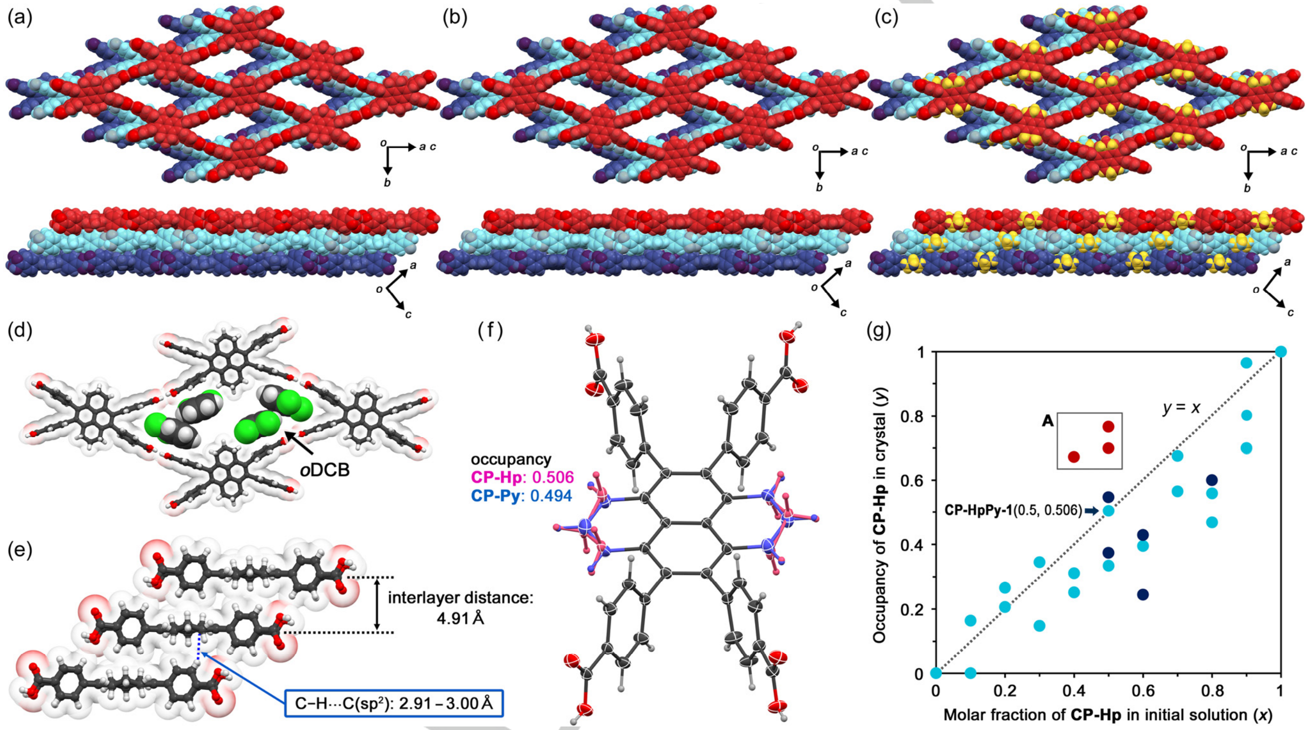

Figure 2. Crystal structures of (a) **CP-Hp-1**, (b) **CP-Py-1**, and (c) cocrystal **CP-HpPy-1**(0.5, 0.506), where yellow-colored parts indicate disordered propylene moieties of hexahydropyrene. (d) Molecules of *o*DCB accommodated in the voids of **CP-Hp-1**. (e) Interlayer contacts in the framework of **CP-Hp-1**. (f) Anisotropic displacement ellipsoid plot for **CP-HpPy-1**(0.5, 0.506), in which the carbon atoms at the 1,2,3- and 6,7,8-positions are disordered in two structures corresponding to **CP-Hp** and **CP-Py**, with occupancies of 0.506 and 0.494, respectively. (g) Composition in single-crystals of **CP-HpPy-1**(*x*, *y*), where *x* and *y* denote the molar fraction or occupancy of **CP-Hp** in the initial solution and the resultant single crystal, respectively. For a certain *x*, the plots in different colors (i.e., cyan and dark blue) indicate that single crystals were selected from different batches. Red circle symbols in box A denote the cocrystals concomitantly obtained with solvate crystals of **CP-Py**.

sheets are slip-stacked to give whole structures of **CP-Hp-1** and **CP-Py-1**. Adjacent pyrene or hexahydropyrene moieties are not pi-stacked each other because of the steric effect of peripheral phenylene groups. For example, the inter-layer distance in **CP-Hp-1** is 4.91 Å (Figure 2e).

To explore the construction of non-stoichiometric cocrystalline frameworks, **CP-Hp** and **CP-Py** were cocrystallized from solutions with the various molar fractions. The obtained single crystals were analyzed crystallographically, and the composition was determined by optimizing the occupancy of the disordered structures.

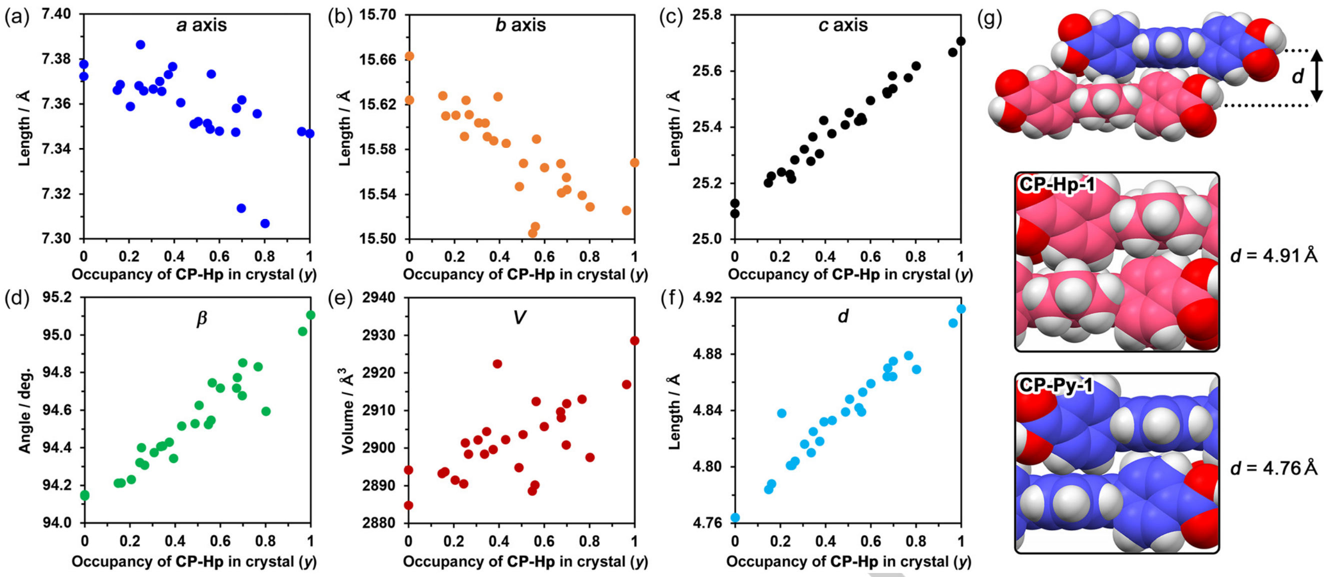

Figure 3. Crystallographic parameters for **CP-HpPy-1** with various y values: (a) *a* axis, (b) *b* axis, (c) *c* axis, (d) angle *β*, (e) cell volume, and (f) intermolecular distance d. (g) Molecular stacking in **CP-HpPy-1** (top) and structural differences between **CP-Hp-1** (center) and **CP-Py-1** (bottom).

A single crystal of the cocrystalline framework is henceforth referred to using the notation **CP-HpPy-1**(x, y) ($0 < x < 1$, $0 < y < 1$), where x and y denote the molar fraction and occupancy of **CP-Hp** in the initial solution and in the resultant single crystal, respectively. Figure 2c shows the crystal structure of **CP-HpPy-1**(0.5, 0.506) as a representative example. The molecular arrangement is nearly the same as those for **CP-Hp-1** and **CP-Py-1**; however, the 1,2,3- and 6,7,8-positions in the pyrene core are disordered because of the coexistence of **CP-Hp** and **CP-Py** molecules, whose occupancy was optimized to be 0.506 and 0.494, respectively (Figure 2f). In total, 26 single crystals obtained from solutions with different mixing ratios or from different batches with the same mixing ratio were analysed. Detailed data for all the crystals are shown in Figure S1 and Table S2.

If **CP-HpPy-1** is an ideal solid-solution crystal, the values of x and y should be uniformly the same. In Figure 2g, the plot shows an approximately proportional relation between the x and y values; more strictly, many of the data points are located in the region $y < x$. This trend is likely due to the greater solubility of **CP-Hp** compared with that of **CP-Py**: their solubility in DMF at 30 °C was determined to be 13.8 and 2.32 mol L^{-1}, respectively. More importantly, the plots show variations among different crystallization batches and even among the same batches with the same composition ratio in the solution. For example, solutions with $x = 0.5$ yielded the following four crystals with different y values: **CP-HpPy-1**(0.5, 0.547), **CP-HpPy-1**(0.5, 0.374), **CP-HpPy-1**(0.5, 0.506), and **CP-HpPy-1**(0.5, 0.334). The former two crystals were picked from one batch, and the other two were from another batch. These results indicate that cocrystallization proceeds in a nonuniform manner, which was also implied by the calculated intermolecular interaction energies (Table S3, Figure S4).

The *x*–*y* balance in **CP-HpPy-1** is also perturbed by precipitation of another crystalline form (Figures S2,S3). When cocrystallization was conducted at lower temperature, another solvate of **CP-Py** [named **CP-Py(DMF)**] was concomitantly precipitated. The formation of **CP-Py(DMF)** consumed **CP-Py**, resulting in increase of the molar fraction of **CP-Hp** in the mother which yielded **CP-HpPy-1** with a y value substantially larger than the corresponding x value, such as **CP-HpPy1**(0.5, 0.767) lying in box A in Figure 2g. Therefore, temperature control is essential.

Notably, the cell parameters for **CP-HpPy-1**(x, y) continuously change from those for **CP-Py-1** to those for **CP-Hp-1** as the y value increases from 0 to 1 (Figure 3). The lengths of the *a* and *b* axes of the unit cell decrease from 7.3723(2) to 7.3469(3) Å and from 15.6634(4) to 15.5682(6) Å, respectively. Similarly, the length of the *c* axis and the *β* angle for the unit cell increase from 25.1288(6) to 25.7065(9) Å and from 94.144(2)° to 95.106(3)°, respectively. The unit-cell volume increases by 1.2%, from 2894.2(1) to 2928.6(2) $Å^3$. These changes are likely attributable to the stacking manner of the molecules. The distance between the two stacked molecules increases as the y value increases from 0 to 1 (Figure 3f). When y is 0 (i.e., **CP-Py-1**), adjacent **CP-Py** molecules are in contact between the sp^2-carbon atom of the pyrene moiety and the peripheral phenylene ring with a C-H···C(sp^2) distance of 2.83–2.85 Å (Figure 3g, bottom). However, when y is 1 (i.e., **CP-Hp-1**), the contact is formed between the methylene parts of the hexahydropyrene moiety and the peripheral phenylene ring, and no contact is observed between the sp^2-carbon atom of the hexahydropynene moiety and the peripheral phenylene ring because of the steric hindrance. The co-crystals have a weighted average structure of **CP-Hp-1** and **CP-Py-1**, which is often observed in solid-solution crystals.[31]

To investigate the effects of the peripheral carboxy phenyl groups on cocrystal formation, the pristine compounds: 1,2,3,6,7,8-hexahydropyrene and pyrene were cocrystallized. They gave intrinsic crystals composed of either compound, instead of cocrystals or solid solutions (Figures S5,S6). These results demonstrate that H-bonding modules play crucial roles in the formation of the non-stoichiometric cocrystalline frameworks.

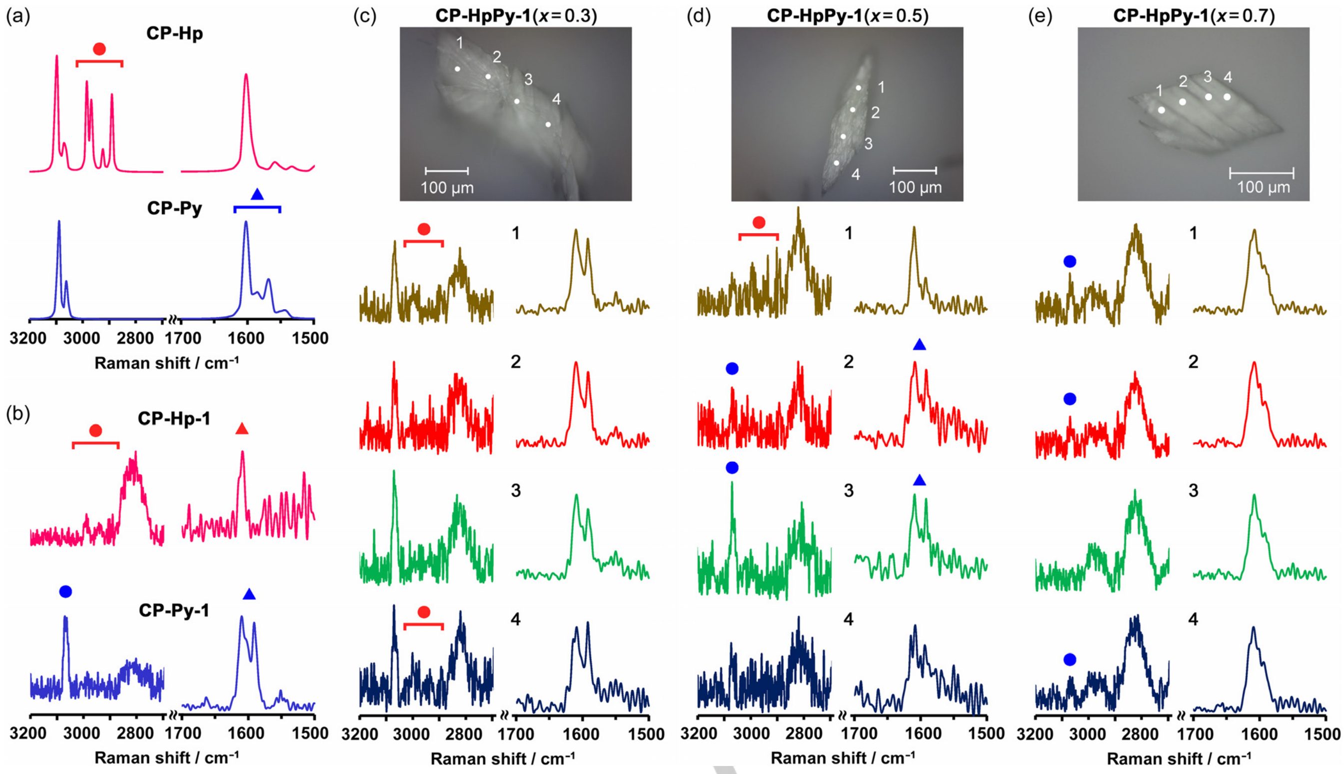

Figure 4. Microscopic Raman spectroscopic analysis of single crystals of the cocrystalline framework **CP-HpPy-1**. (a) Theoretical spectra for molecules of **CP-Hp** and **CP-Py** calculated at the DFT B3LYP/6-31G(d) level. (b) Observed spectra of single crystals of **CP-Hp-1** and **CP-Py-1**. Observed spectra of single crystals of (c) **CP-HpPy-1**(x = 0.3), (d) **CP-HpPy-1**(x = 0.5), and (e) **CP-HpPy-1**(x = 0.7), where spectra 1, 2, 3, and 4 were recorded at different positions numbered on the photographs of the single crystal shown at the top.

To determine whether molecules of **CP-Hp** and **CP-Py** are distributed uniformly or inhomogeneously in the crystals, microscopic FT-IR and Raman spectroscopy were conducted on single crystals of the frameworks (Figures 4 and S7–S10). Particularly, Raman spectroscopy provided precise information about the component distribution in the cocrystals. The excitation wavelength was 532 nm, which was not overlapped with UV-vis absorption bands of either **CP-Hp** or **CP-Py** to allow quantitative comparison of the peaks. The beam spot size for the measurement was approximately 1 μm. Theoretical spectrum of **CP-Hp** shows several prominent peaks in 2900–3100 cm^{-1} and a sharp signal at 1602 cm^{-1}, whereas that of **CP-Py** shows peaks in 3071–3097 cm^{-1} and split bands in 1568–1602 cm^{-1} (Figure 4a). In the experimental spectrum of a single crystal of **CP-Hp-1**, the predicted peaks in 2900–3100 cm^{-1} (marked with a red solid circle) appear with weak intensity. In addition, a broad band at 2800 cm^{-1}, which does not appear in the calculated spectrum for the molecule, was observed, and is likely due to a packing effect in the crystal (Figure 4b, top). In the case of **CP-Py-1**, the predicted peaks are well reproduced in the observed spectrum; they are marked by a blue circle and triangle (Figure 4b, bottom). We therefore conducted characterization of cocrystals **CP-HpPy-1** on the basis of these characteristic peaks as follows. Raman spectra were recorded at different four positions in each single crystal of **CP-HpPy-1**(x = 0.3), **CP-HpPy-1**(x =0.5), and **CP-HpPy-1**(x = 0.7) (Figure 4c–e). In the spectrum of **CP-HpPy-1**(x = 0.3), the most characteristic peaks are ascribable to **CP-Py**, although weak but clearly discernible peaks due to **CP-Hp** are observed with different intensities in 2900–3100 cm^{-1} (e.g., see signals marked with a red solid circle in the spectra corresponding to positions 1 and 4). In the case of **CP-HpPy-1**(x = 0.5), differences in the spectra recorded at four positions are more prominent: the spectrum corresponding to position 1 mainly shows peaks due to **CP-Hp**, whereas that corresponding to position 3 shows predominantly **CP-Py** peaks, and the peaks at the other two positions are spectral features of both compounds. Similarly, in the case of **CP-HpPy-1**(x = 0.7), no clear contribution of **CP-Py** was observed in the spectrum corresponding to position 3. These results indicate that single crystals of the cocrystalline framework **CP-HpPy-1** are not composed of homogenously distributed **CP-Hp** and **CP-Py** molecules but have gradational and/or inhomogeneous composition ratio (Figure 5). This is

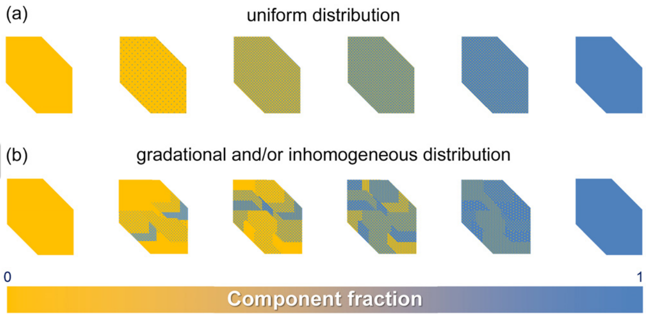

Figure 5. Schematic of (a) ideal solid-solution crystal and (b) cocrystal with gradational and/or inhomogeneous distribution of components, latter of which is considered to form in the present study.

consistent with the observed nonuniform co-crystallization behavior.

Fluorescence spectra of crystalline bulk samples of **CP-Py-1**, **CP-Hp-1**, and **CP-HpPy-1**(x = 0.5) were measured (Figure 6). The spectrum of **CP-Hp-1** shows a broad fluorescence band at 389 nm with a quantum yield (Φ_F) of 0.035, whereas that of **CP-Py-1** shows clear vibration structures at 402, 423, and 450 nm (Φ_F = 0.11). **CP-HpPy-1**(x = 0.5) shows fluorescence bands at 383, 402, and 423 nm with Φ_F of 0.055. These bands are ascribable to those of **CP-Hp-1** and **CP-Py-1**, although a band with the highest energy was sharped and slightly blue-shifted in the case of **CP-HpPy-1**(x = 0.5).

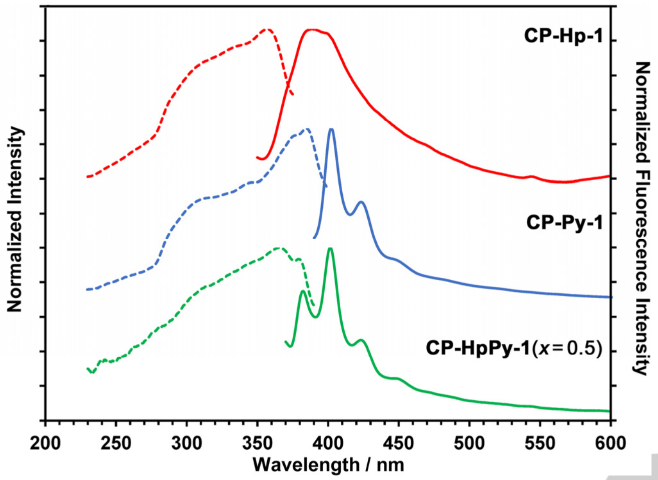

Figure 6. Solid-state fluorescence (solid line) and excitation (dashed line) spectra of **CP-Hp-1**, **CP-Py-1**, and **CP-PyHy-1**(x = 0.5). λ_{ex} = 320, 353, and 350 nm, respectively; λ_{em} = 401, 420, and 430 nm, respectively.

Conclusion

Structurally precise non-stoichiometric cocrystalline HOFs were developed from hydropyrene and pyrene derivatives **CP-Hp** and **CP-Py** possessing four carboxy groups. The frameworks were constructed through networking by directional hydrogen bonding of peripheral carboxy groups. The precise composition and structure of the cocrystalline frameworks was determined on the basis of single-crystal X-ray diffraction analysis. Furthermore, microscopic Raman spectroscopy on a single crystal of the frameworks firstly indicates that they are not ideal solid solutions with the uniform distribution of the components but are non-stoichiometric cocrystal with gradational and/or inhomogeneous distribution. These results are important for the development of new functional porous materials with nonstoichiometric components.

Acknowledgements

This work is supported by KAKENHI (JP21K18961, JP21H01919, JP21H05485, and JP22H05461) from JSPS and MEXT Japan. I.H. thanks Tokuyama Science Foundation, Hoansha Foundation, and Nagase Science and Technology Foundation for their financial support. I.H. also thanks the Multidisciplinary Research Laboratory System for Future Developments (MRL), Graduate School of Engineering Science, Osaka University. The authors thank the Cybermedia Center, Osaka University, for use of the Supercomputer for Quest to Unsolved Interdisciplinary Datascience (SQUID). The authors acknowledge Ms. R. Miyake for HR-MS analysis. The authors deeply appreciate the reviewers for fruitful comments.

Keywords: solid solution • cocrystal • hydrogen-bonded framework • reticular chemistry • crystal engineering

[1] Q. Zhang, K. Kusada, D. Wu, T. Yamamoto, T. Toriyama, S. Matsumura, S. Kawaguchi, Y. Kubota, H. Kitagawa, *J. Am. Chem. Soc.* **2022**, *144*, 4224–4232.
[2] D. N. Bunck W. R. Dichtel, *Chem. Eur. J.* **2013**, *19*, 818–827.
[3] M. Lusi *CrystEngComm* **2018**, *20*, 7042–7052.
[4] T. Miyano, I. Hisaki, N. Tohnai, N. *Chem. Lett.* **2017**, *46*, 225–227.
[5] M. Dabros. P. R. Emery, V. R. Thalladi, *Angew. Chem. Int. Ed.* **2007**, *46*, 4132–4135; *Angew. Chem.* **2007**, *119*, 4210–4213.
[6] D.-K. Bučar, A. Sen, S. V. Santhana Mariappan, L. R. MacGillivray, *Chem. Commun.* **2012**, *48*, 1790–1792.
[7] M. Paul, S. Chakraborty, G. R. Desiraju, *J. Am. Chem. Soc.* **2018**, *140*, 2309–2315.
[8] N. Juneja, N. M. Shapiro, D. K. Unruh, E. Bosch, R. H. Groeneman, K. M. Hutchins, *Angew. Chem. Int. Ed.* **2022**, e202202708; *Angew. Chem.* **2022** e 202202708.
[9] H. Deng, C. J. Doonan, H. Furukawa, R. B. Ferreira, J. Towne, C. B. Knobler, B. Wang, O. M. Yaghi, *Science* **2010**, *327*, 846–850.
[10] R. L. Li, A. Yang, N. C. Flanders, M. T. Yeung, D. T. Sheppard, W. R. Dichtel, *J. Am. Chem. Soc.* **2021**, *143*, 7081–7087.
[11] O. Bolton, K. Lee, H.-J. Kim, K. Y. Lin, J. Kim, *Nat. Chem.* **2011**, *3*, 205–210.
[12] Bolla, B. Sarma, A. K. Nangia, *Chem. Rev.* **2022**, *122*, 11514–11603.
[13] J. Luo, J.-W. Wang, J.-H. Zhang, S. Lai, D.-C. Zhong, *CrystEngComm* **2018**, *20*, 5884–5898.
[14] R.-B. Lin, Y. He, P. Li, H. Wang, W. Zhou, B. Chen, *Chem. Soc. Rev.* **2019**, *48*, 1362–1389.
[15] I. Hisaki, C. Xin, K. Takahashi, T. Nakamura, *Angew. Chem. Int. Ed.* **2019**, 58, 11160−11170; *Angew. Chem.* **2019**, 131, 11278−11288.
[16] B. Wang, R.-B. Lin, Z. Zhang, S. Xiang, B. Chen, *J. Am. Chem. Soc.* **2020**, 142, 14399−14416.
[17] P. Li, M. R. Ryder, J. F. Stoddart, *Acc. Mater. Res.* **2020**, *1*, 77–87.
[18] X. Song, Y. Wang, C. Wang, D. Wang, G. Zhuang, K. O. Kirlikovali, P. Li, O. K. Farha, *J. Am. Chem. Soc.* **2022**, *144*, 10663−10687.
[19] R. E. Melendez, C. V. K. Sharma, M. J. Zaworotko, C. Bauer, R. D. Rogers, *Angew. Chem., Int. Ed. Engl.* **1996**, *35*, 2213–2215.
[20] J. Lü, C. Perez-Krap, M. Suyetin, N. H. Alsmail, Y. Yan, S. Yang, W. Lewis, E. Bichoutskaia, C. C. Tang, A. J. Blake, R. Cao, M. Schröder, *J. Am. Chem. Soc.* **2014**, *136*, 12828–12831.
[21] T. Adachi, M. D. Ward, *Acc. Chem. Res.* **2016**, *49*, 2669–2679.
[22] M. Morshedi, M. Thomas, A. Tarzia, C. J. Doonan, N. G. White, *Chem. Sci.* **2017**, *8*, 3019–3025.
[23] Y.-H. Luo, X.-T. He, D.-L. Hong, C. Chen, F.-H. Chen, J. Jiao, L.-H. Zhai, L.-H. Guo, B.-W. Sun, *Adv. Funct. Mater.* **2018**, *28*, 1804822.
[24] R. Liang, J. Samanta, B. Shao, M. Zhang, R. J. Staples, A. D. Chen, M. Tang, Y. Wu, I. Aprahamian, C. Ke, *Ang. Chem. Int. Ed.* **2021**, *60*, 23176–23181; *Angew. Chem.* **2021**, *133*, 23360–23365.
[25] Q. Chen, T. Zhang, X. Chen, M. Liang, H. Zhao, P. Yuan, Y. Han, C.-P. Li, J. Hao, P. Xue, *ACS Appl. Mater. Interfaces* **2022**, *14*, 24509–24517.
[26] I. Hisaki, S. Nakagawa, N. Tohnai, M. Miyata, *Angew. Chem. Int. Ed.* **2015**, *54*, 3008–3012; *Angew. Chem.* **2015**, *127*, 3051–3055.
[27] I. Hisaki, S. Nakagawa, N. Ikenaka, Y. Imamura, M. Katouda, M. Tashiro, H. Tsuchida, T. Ogoshi, H. Sato, N. Tohnai, M. Miyata, *J. Am. Chem. Soc.* **2016**, *138*, 6617–6628.
[28] I. Hisaki, Y. Suzuki, E. Gomez, Q. Ji, N. Tohnai, T. Nakamura, A. Douhal, *J. Am. Chem. Soc.* **2019**, *141*, 2111–2121.

[29] Z. Lu, R. Wang, Y. Liao, O. K. Farha, W. Bi, T. R. Sheridan, K. Zhang, J. Duan, J. Liu, J. T. Hupp, *Chem. Commun.* **2021**, *57*, 3571–3574.

[30] Deposition numbers 2206158 (for **CP-Hp-1**), 2206159 (for **CP-Py-1**), 2206160 (for **CP-HpPy-1**(0.5, 0.506), 2206161 (for **CP-Py(DMF)**) contain the supplementary crystallographic data for this paper. These data are provided free of charge by the joint Cambridge Crystallographic Data Centre and Fachinformationszentrum Karlsruhe Access Structures service.

[31] K. Sada, K. Inoue, T. Tanaka, A. Epergyes, A. Tanaka, N. Tohnai, A. Matsumoto, M. Miyata, *Angew. Chem. Int. Ed.* **2005**, *44*, 7059–7062; *Angew. Chem.* **2005**, *117*, 7221–7224.

Entry for the Table of Contents

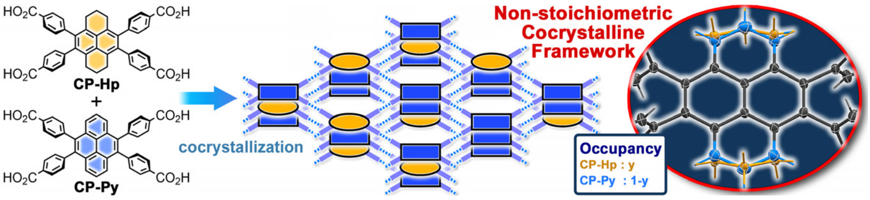

Proof-of-concept non-stoichiometric cocrystalline frameworks are formed using hexahydropyrene and pyrene derivatives with hydrogen-bonding modules, **CP-Hp** and **CP-Py**. The structures and composition ratio were determined by single-crystal X-ray diffraction. Microscopic Raman spectroscopy on a single crystal showed that components are distributed gradationally and/or not homogenously in the crystal.

Institute and/or researcher Twitter usernames: @HisakiLab